ANALYSIS OF MSD CRACK GROWTH IN MECHANICALLY FASTENED FIBRE METAL LAMINATE JOINTS

Wandong Wang[1], Calvin Rans[2], Zhinan Zhang[3], Rinze Benedictus[4]

[1]Faculty of Aerospace Engineering, Delft Univeristy of Technology, Delft, the Netherlands
Email: W.Wang-3@tudelft.nl, Web Page:https://www.linkedin.com/in/wandong-wang-785346a7
[2]Faculty of Aerospace Engineering, Delft Univeristy of Technology, Delft, the Netherlands
Email: C.D.Rans@tudelft.nl, Web Page: http://calvinrans.com
[3]The First Aircraft Design and Research Institute of AVIC, Xi′an, China
Email: zhangzhinan198678@126.com
[4]Faculty of Aerospace Engineering, Delft Univeristy of Technology, Delft, the Netherlands
Email: R.Benedictus@tudelft.nl, Web Page: http://staff.tudelft.nl/en/R.Benedictus

Keywords: MSD, fibre metal laminate, mechanically fastened joints, superposition, fatigue crack growth

Abstract
In the light of the introduction of Limit of Validity to the airworthiness regulations, it is crucial to examine the MSD behaviour of damage tolerant FML structures. This paper outlines a prediction model for analysing MSD crack growth in mechanically fastened joints based on linear elastic fracture mechanics and the principle of superposition. Test data on a Glare lap joint from open literature is used to verify the proposed model. As a first approximation for lap joints, the prediction model without considering secondary bending effects on crack growth behaviour in FMLs provides conservative prediction results compared to the test results for a FML lap joint where secondary bending could exacerbate loading in the faying layer.

1. Introduction

Fibre metal laminates (FMLs) are a class of hybrid materials that consist of alternating layers of monolithic metallic sheet and fibre prepreg. Although FMLs can be categorized as composite materials, they exhibit metal-like behavioural features [1], such as slow fatigue cracking in the metal layers of FMLs. FMLs take advantage of the merits of both the metal and composite constituents exhibiting superior resistance to fatigue cracking under cyclic loading. The fatigue resistant composite layers remain intact in the wake of fatigue cracks in the metal layers and provide an extra load path for cracked metal layers. The load transfer from the cracked metal layers of FMLs to the composite layer is called bridging mechanism (Fig. 1) and results in reduced driving force for the crack growth in the metal layers [2]. Therefore FMLs are regarded as damage tolerant materials with the feature of slow damage growth, which is very desirable in the aerospace sector.

The damage tolerance models for FMLs mainly focus on the growth behaviour of an isolated fatigue damage, they simultaneously predict the fatigue cracking in the metallic sheets and coupled delamination growth at the metal/composite interfaces of FMLs [2]. However, the damage tolerance models can be invalidated due to the simultaneous appearance of multiple-site fatigue damages in a FML structure. In the light of the new Limit of Validity requirement which places limits on the damage tolerance phi-

Excerpt from ISBN 978-3-00-053387-7

losophy, it is crucial to examine the fatigue crack growth behaviour in damage tolerant FML structures with MSD scenario [3, 4].

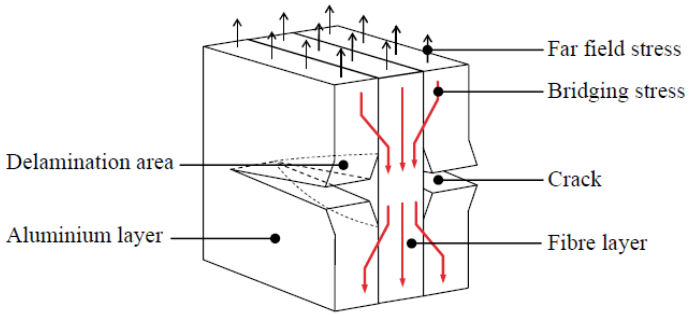

Figure 1. Illustration of bridging mechanism.

This paper analyses the MSD crack growth behaviour in mechanically fastened FML joints that are susceptible to MSD cracking starting from hole edges. Several mechanisms are involved in such phenomena: load transfer in the joints, non-symmetric crack growth and delamination growth of each damage state, the interaction between MSD cracks and pin-bearing effects. An analysis methodology incorporating these phenomena is proposed in this paper and is verified with test data from open literature.

The effects of secondary bending on the crack growth behaviour in FMLs are not modelled in the proposed methodology in this paper. This would not be problematic for double lap joints where secondary bending is absent. Whereas secondary bending occurs in single lap joints and aggravates loading case for the faying layer. Test results of a Glare lap joint from literature are compared to the prediction results to show the validity of the model for the case where secondary bending occurs.

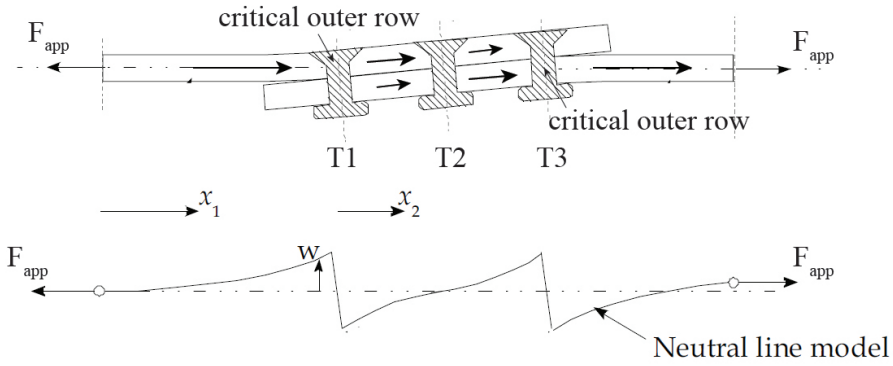

Figure 2. Illustration of load transfer and secondary bending due to eccentric load path.

2. Model implementation

In a mechanically fastened joint, load transfers from one panel to another panel through fasteners, such as solid rivets and bolts. Secondary bending can also arise in a lap-splice joint at the outer rivet rows as a result of the eccentric load path in the joint (see Fig. 2), exacerbating the loading in the faying layer.

Excerpt from ISBN 978-3-00-053387-7

In a lap-splice joint illustrated in Fig. 2, the load transfer in different rivet rows can be calculated neglecting the load transferred by friction [5]:

$$T1 = \frac{f_{rivet} + f_{sheet}}{3 \cdot f_{rivet} + 2 \cdot f_{sheet}} \cdot F_{app}. \tag{1}$$

$$T2 = \frac{f_{rivet}}{3 \cdot f_{rivet} + 2 \cdot f_{sheet}} \cdot F_{app}. \tag{2}$$

where $T1$ and $T2$ are respective loads transferred by the first rivet row and second rivet row. f_{rivet} is empirically determined rivet flexibility and f_{sheet} is sheet flexibility [5]. $T3$ in the third rivet row is equal to $T1$ from the symmetry point of view for the joint. The details of calculating load transfer in a FML joint can be found in [5].

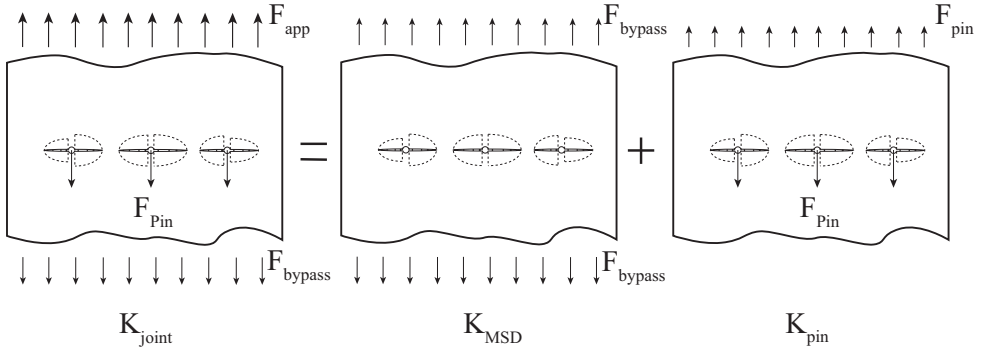

Figure 3. Superposition scheme of the stress intensity factor for MSD cracks in a joint.

This paper applies linear elastic fracture mechanics (LEFM) to address MSD crack growth in mechanically fastened FML joints. From this point of view, the stress intensity factor (SIF) of a crack tip can be decomposed into SIFs resulted from different loading cases for which the SIF solutions can be derived. Fig. 3 illustrates the scheme of superposition for calculating stress intensity factor with LEFM in order to analyse MSD crack growth in a joint. For a critical row containing MSD cracks in a FML joint, the stress intensity factor, K_{joint}, for a crack tip is superposed by the stress intensity factor, K_{MSD}, resulted from the by-pass loading and the stress intensity factor, K_{pin}, due to pin bearing.

$$K_{joint} = K_{MSD} + K_{pin}. \tag{3}$$

The assumption made for calculating MSD crack growth in this paper is that the by-pass loading and pin loading do not change as cracks grow. The following subsections give the essentials for analysing the SIFs under by-pass loading and pin loading respectively. Secondary bending effects are not considered in this model.

2.1. Analysis of crack states in a FML with MSD cracks under by-pass loading

The by-pass loading can be regarded as far-field loading in the analysis of the crack states in a FML containing MSD cracks (Fig. 3). In [4], it has been explained that simultaneously predicting all crack states of a FML containing MSD cracks is not practical. A simplified analysis methodology therefore

Excerpt from ISBN 978-3-00-053387-7

has been proposed based on the nature of fatigue in FMLs: the presence of adjacent cracks are idealized as reduction in local stiffness to evaluate the load transfer from the adjacent cracks to a single crack, the influence of adjacent cracks on a single crack can therefore be estimated and this process can be repeated until all the crack states are calculated (see Fig. 4) [4].

The Westergaard stress distribution is applied to describe the stress distribution in front of a crack tip in a FML [3]. The presence of a crack in front the crack tip is idealized as a negative stiffener, indicating that the location of the crack is modeled as removal of metal strips [3]. Consequently, the stress distribution is changed in the presence of additional cracks, the Westergaard stress distribution is not smooth but with less magnitude at the crack locations with the assumption of isostrain between crack locations and surrounding laminate material, which is illustrated in Fig. 4. For the detailed calculation of the stress distribution with a negative stiffener, one can refer to [3].

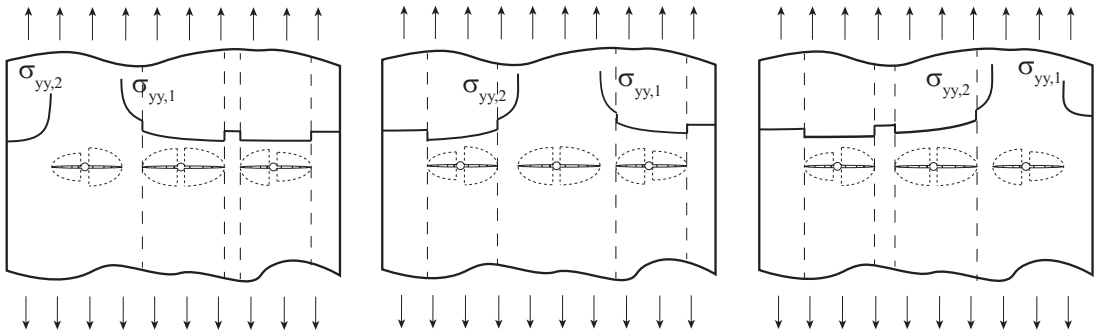

Figure 4. Illustration of sequential analysis of each crack state.

As schematically illustrated in Fig. 4, the non-symmetry leads to non-symmetric stress distributions in front of two crack tips of a single crack. In order to address the non-symmetry, the load balance (Eq. 4) and moment balance (Eq. 5) should be carried out simultaneously.

$$\int \sigma_{yy,1} + \int \sigma_{yy,2} = F_{far-field} \tag{4}$$

$$d_1 \int \sigma_{yy,1} = d_2 \int \sigma_{yy,2} \tag{5}$$

with $F_{far-field}$ being the far-field load. d_1, d_2 are the distances from the centroids of two stress distributions to the middle of the panel.

According to the Westergaard stress functions, the crack opening displacement (COD) solution resulted from the Westergaard stress distribution describes a half crack with a maximum crack opening at the root ($x = 0$) [6]. For a non-symmetric crack, its COD is obtained via implementing identical crack opening at the roots of two half cracks described by the two different Westergaard stress distributions. The principle of displacement compatibility used by Alderliesten can be applied to calculate the bridging stress distribution, and then stress intensity factor shielding due to the bridging stress (K_{br}) can also be calculated [2]. In the MSD scenario, the delamination shapes on both sides of a crack can be asymmetric, the Westergaard stress functions on Page 5.6 in [7] has to be used to carry out the mentioned calculation here.

Excerpt from ISBN 978-3-00-053387-7

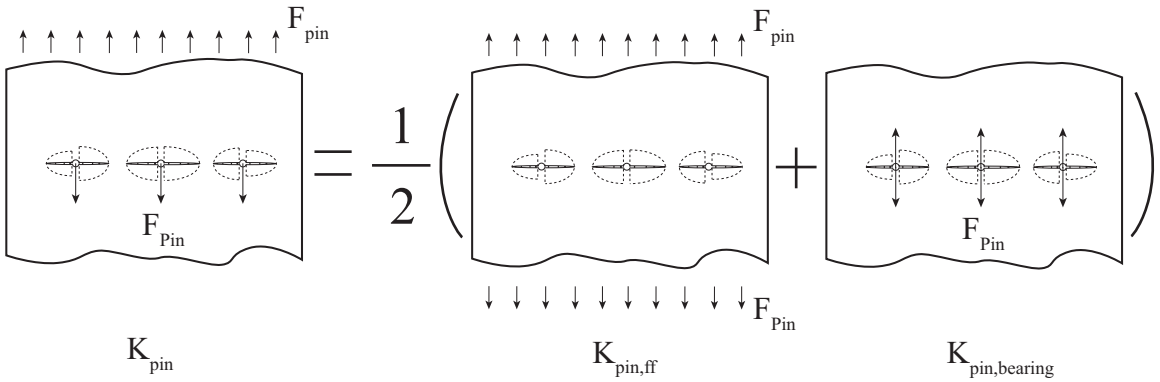

Figure 5. Illustration of superposition for pin-loading case.

The resulted stress intensity factor (K_{MSD}) for the crack tip of a single crack is given as follows [7]:

$$K_{MSD} = K_{ff} - K_{br} \tag{6}$$

where K_{ff} is the stress intensity factor resulted from the far-field load and load redistribution which is introduced by the presence of other cracks.

2.2. Analysis of crack states in a FML with pin-loading effects

In order to calculate K_{pin} illustrated in Fig. 3, the superposition method shown in Fig. 5 is employed (see Eq. 7). The methodology given in the preceding subsection can be used to analyse $K_{pin,ff}$.

$$K_{pin} = \frac{1}{2}K_{pin,ff} + \frac{1}{2}K_{pin,bearing} \tag{7}$$

The pin bearing load for a crack in a joint is simplified as a point load in this paper. Compared to the stress distribution in front of a crack tip in a metal panel under tensile stress, the stress distribution of the crack loaded by a pair of point loads has much lower magnitude millimeters away from its crack tip. One example of these two stress distributions for respective loading cases is given in Fig. 6.

For the calculation of $K_{pin,bearing}$ illustrated in (Fig. 5), the crack interaction effects are neglected since the reduction in the stiffness caused by the presence of MSD cracks introduces very small quantity of load redistribution in comparison with the load redistribution under the far-field stress loading. Each crack is analyzed separately as an isolated crack loaded by a pair of point loads.

It is assumed that the fibres cut at the pin hole do not carry pin loading, it is only the metal layers that carry the load. The fibres in the wake of fatigue crack carries the load via constraining the crack opening displacement introduced by the pin-loading.

The stress intensity factors for a crack in a metal layer loaded by a pair of pin loads depicted in Fig. 7 is given by:

Excerpt from ISBN 978-3-00-053387-7

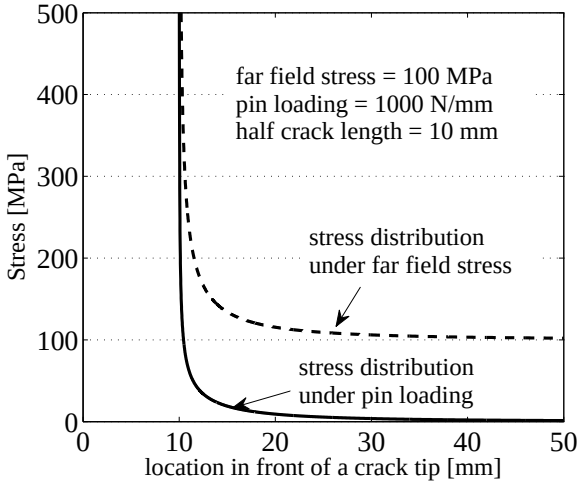

Figure 6. Stress distributions under far field stress and under point loading.

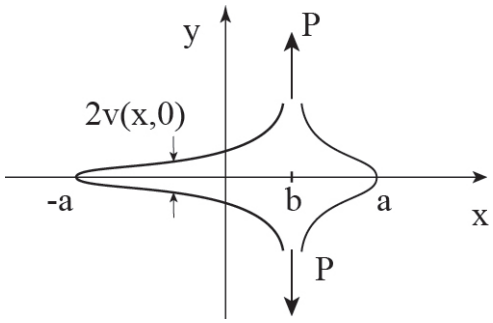

Figure 7. symmetric point load case from [7].

$$K_{P\pm a} = \frac{P}{\sqrt{\pi a}} \frac{\sqrt{a^2 - b^2}}{a \mp b} \tag{8}$$

where P is equal to F_{pin} divided by the total thickness of metal layers. And the crack opening displacement is as follows:

$$2v\,(x,0) = \frac{4P}{\pi E} cosh^{-1} \frac{a^2 - bx}{a|x - b|} \tag{9}$$

with E being the Young's modulus.

Again the bridging mechanism should be considered. The stress intensity factor caused be the bridging stress in the bridging fibres, $K_{br,pin}$, can also be derived with the Westergaard stress functions given on Page 5.6 in crack analysis handbook [7]. $K_{pin,bearing}$ is then given by:

$$K_{pin,bearing} = K_P - K_{br,pin} \tag{10}$$

Excerpt from ISBN 978-3-00-053387-7

With the stress intensity factors for different loading cases known, the Eq. 3 can be used for calculating the superposed stress intensity factor for each crack tip. The crack growth can then be predicted with a Paris relationship used by Alderliesten [2]. The calculated bridging stresses can also be superposed and be used to calculate the strain energy release rate, G, at the interface between metal layers and fibre layers. The delamiantion growth can also be predicted then with G known. Detailed calculation can be referred to [2].

3. Model validation

Müller studied the fatigue behaviour of Glare riveted lap joints [8]. Results of test series 4 from the study of fatigue behaviour of Glare3 riveted lap joints were selected for the validation of the proposed model. The test series consisted of two Glare3-3/2-0.3 sheets jointed with three rows of rivets (see the inset in Fig. 8) while each row had three rivets. The width of Glare3 sheet was 72 mm.

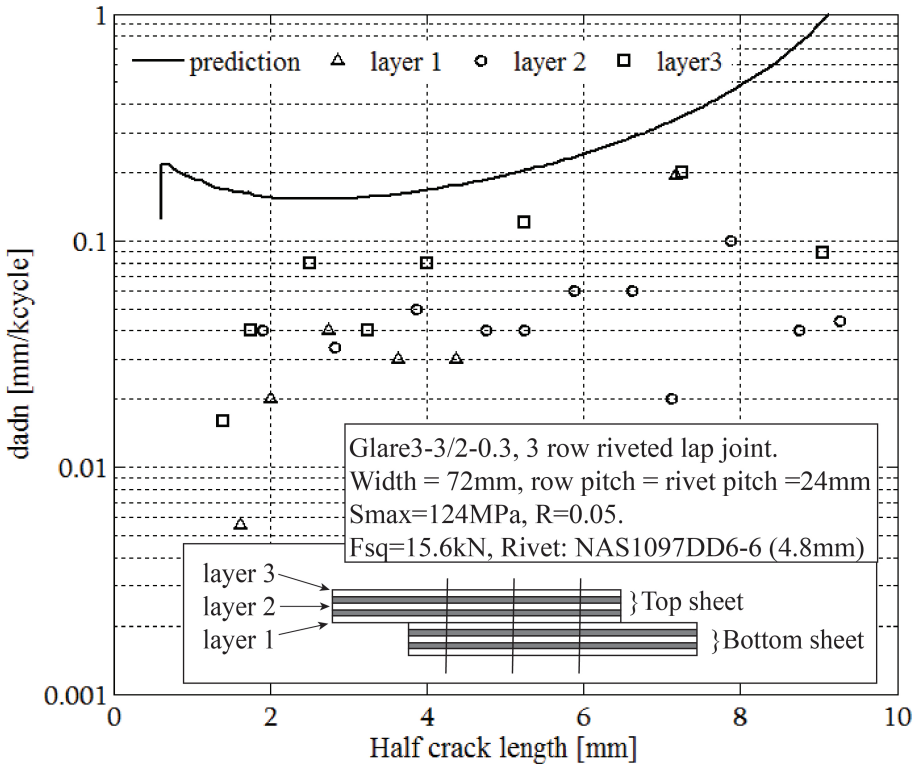

Figure 8. Comparison of crack growth rates of 3 layers in the top sheet.

The compiled crack growth rates in the metal layers of the top sheet in a joint riveted with squeeze force of 15.6 kN, including the prediction results for through thickness cracks from the proposed analysis model, are given in Fig. 8. Crack growth only measured for the central rivet in the critical row with eddy current non-destructive inspection technique. The accuracy of the test data is limited because the inspection method for invisible cracks is poor [8] and the obtained data points are few. Layer 1 has the highest tensile stress due to bending effects, however the crack growth in the beginning is very slow as a result of beneficial residual stress from high riveting squeeze force and the bridging mechanism provided by fibre layers and intact layer 2 and 3 (larger crack free life due to secondary bending). Layer 3 has the highest crack growth rate due to the fact that layer 1 is completely cracked and layer 2 is partially cracked. However, compressive bending stress resulted both from eccentric load paths in the joint and

Excerpt from ISBN 978-3-00-053387-7

in the eccentrically cracked laminate may play a beneficial role in constraining the crack growth rate in layer 3.

The analysis model does not take the effects of squeeze force and secondary bending into consideration, it is assumed that the crack initiates in all metal layers simultaneously. The predicted crack growth rate is high in the beginning due to the pin-loading effects. It decreases with crack growth since the pin-loading effects are becoming weaker. The crack interaction accelerates the crack growth in the end. Compared to the test data, the prediction model as a first approximation gives conservative results for a lap splice joint where secondary bending occurs.

4. Conclusion

The proposed analysis methodology for MSD crack growth prediction in mechanically fastened FML joints is based on LEFM. The principle of superposition is applied to decompose the stress intensity factor of cracks in a joint into several items pertaining to respective loading cases involved in a joint. Crack interaction is simplified as load redistribution mechanism by modeling adjacent cracks as negative stiffeners. As a first approximation for lap joint, the bending effects are not considered.

Based on the comparison of crack growth rates, the proposed analysis model provides conservative prediction results for FML lap joints where secondary bending effects arise. The bridging mechanism alleviates the adverse effects posed by secondary bending on the crack growth in the faying layer in a FML lap joint. Double shear lap joints can be tested to further verify the prediction model.

References

[1] C. D. Rans. 2 - bolted joints in glass reinforced aluminium (glare) and other hybrid fibre metal laminates (fml). *in Composite Joints and Connections*, 2011.

[2] R. C. Alderliesten. Analytical prediction model for fatigue crack propagation and delamination growth in glare. *International Journal of Fatigue*, 29(4):628–646, 2007.

[3] W. Wang, C. Rans, R. C. Alderliesten, and R. Benedictus. Predicting the influence of discretely notched layers on fatigue crack growth in fibre metal laminates. *Engineering Fracture Mechanics*, 145:1–14, 2015.

[4] W. Wang, C. Rans, R.C. Alderliesten, and R. Benedictus. Philosophy of multiple-site damage analysis for fibre metal laminate structures. *Proceedings of 28th Symposium of the International Committee on Aeronautical Fatigue ICAF 2015, Helsinki, Finland*, June 1-5 2015.

[5] J. J. M. De Rijck. *Stress analysis of fatigue cracks in mechanically fastened joints: an analytical and experimental investigation*. PhD thesis, Delft University of Technology, 2005.

[6] H.M. Westergaard. Bearing pressure and cracks. *Journal of Applied Mechanics*, 6:49–53, 1939.

[7] H. Tada, P. C. Paris, and G. R. Irwin. *The stress analysis of cracks handbook*. ASME, New York, 2000.

[8] R. P. G. Müller. *An experimental and analytical investigation on the fatigue behaviour of fuselage riveted lap joints : the significance of the rivet squeeze force, and a comparison of 2024-T3 and glare 3*. PhD thesis, Delft University of Technology, 1995.

Excerpt from ISBN 978-3-00-053387-7